

receptor *EphB4* and its specific transmembrane ligand *ephrin-B2* in cardiovascular development. *Mol. Cell* **4**, 403–414 (1999).

16. Shalaby, F. *et al.* Failure of blood-island formation and vasculogenesis in Flk-1-deficient mice. *Nature* **376**, 62–66 (1995).

17. Kawasaki, T. *et al.* A requirement for neuropilin-1 in embryonic vessel formation. *Development* **126**, 4895–4902 (1999).

18. Zhong, T. P., Childs, S., Leu, J. P. & Fishman, M. C. Gridlock signalling pathway fashions the first embryonic artery. *Nature* **414**, 216–220 (2001).

19. Fischer, A., Schumacher, N., Maier, M., Sendtner, M. & Gessler, M. The Notch target genes *Hey1* and *Hey2* are required for embryonic vascular development. *Genes Dev.* **18**, 901–911 (2004).

20. Garcia-Porrero, J. A., Godin, I. E. & Dieterlen-lievre, F. Potential intraembryonic hemogenic sites at pre-liver stages in the mouse. *Anat. Embryol. (Berl.)* **192**, 427–435 (1995).

21. Taviani, M. *et al.* Aorta-associated CD34<sup>+</sup> hematopoietic cells in the early human embryo. *Blood* **87**, 67–72 (1996).

22. Medvinsky, A. L., Samoylina, N. L., Muller, A. M. & Dzierzak, E. A. An early pre-liver intraembryonic source of CFU-S in the developing mouse. *Nature* **364**, 64–67 (1993).

23. Godin, I. E., Garcia-Porrero, J. A., Coutinho, A., Dieterlen-lievre, F. & Macros, M. A. Para-aortic splanchnopleura from early mouse embryos contains B1a cell progenitors. *Nature* **364**, 67–69 (1993).

24. Zhang, J. *et al.* Identification of the haematopoietic stem cell niche and control of the niche size. *Nature* **425**, 836–841 (2003).

25. Calvi, L. M. *et al.* Osteoblastic cells regulate the haematopoietic stem cell niche. *Nature* **425**, 841–846 (2003).

26. Hogan, B. L. M., Beddington, R. S. P., Costantini, E. & Lacy, E. *Manipulating the Mouse Embryo, a Laboratory Manual* (Cold Spring Harbor Laboratory Press, New York, 1994).

27. Adams, R. H. Molecular control of arterial-venous blood vessel identity. *J. Anat.* **202**, 105–112 (2003).

Supplementary Information accompanies the paper on [www.nature.com/nature](http://www.nature.com/nature).

**Acknowledgements** We thank W. Qian and C. Yang for technical assistance; M. Yanagisawa for providing the *Tie2-Cre* transgenic mice; Y. Furuta for providing the *Efnb2* construct for RNA *in situ* hybridization; and F. Petit for the *COUP-TFII* minigene construct. We also thank L.-Y. Yu-Lee and H. J. Bellen for discussions and critical reading of the manuscript. This work was supported by NIH grants to S.Y.T. and M.-J.T.

**Competing interests statement** The authors declare that they have no competing financial interests.

**Correspondence** and requests for materials should be addressed to S.Y.T. (stsai@bcm.tmc.edu) or M.-J.T. (mtsai@bcm.tmc.edu).

## LPA<sub>3</sub>-mediated lysophosphatidic acid signalling in embryo implantation and spacing

Xiaoqin Ye<sup>1\*</sup>, Kotaro Hama<sup>2\*</sup>, James J. A. Contos<sup>4</sup>, Brigitte Anliker<sup>1</sup>, Asuka Inoue<sup>2</sup>, Michael K. Skinner<sup>5</sup>, Hiroshi Suzuki<sup>3,6</sup>, Tomokazu Amano<sup>3</sup>, Grace Kennedy<sup>1</sup>, Hiroyuki Arai<sup>2</sup>, Junken Aoki<sup>2</sup> & Jerold Chun<sup>1</sup>

<sup>1</sup>Department of Molecular Biology, Helen L. Dorris Child and Adolescent Neuropsychiatric Disorder Institute, The Scripps Research Institute, 10550 North Torrey Pines Road, La Jolla, California 92037, USA

<sup>2</sup>Graduate School of Pharmaceutical Sciences, and <sup>3</sup>Department of Developmental Medical Technology (Sankyo), Graduate School of Medicine, University of Tokyo, 7-3-1, Hongo, Bunkyo-ku, Tokyo 113-0033, Japan

<sup>4</sup>Fred Hutchinson Cancer Research Center, 1100 Fairview Avenue North, Seattle, Washington 98109-1024, USA

<sup>5</sup>Center for Reproductive Biology, School of Molecular Bioscience, Washington State University, Pullman, Washington 99164-4231, USA

<sup>6</sup>National Research Center for Protozoan Diseases, Obihiro University of Agriculture and Veterinary Medicine, Obihiro 080-8555, Japan

\* These authors contributed equally to this work

**Every successful pregnancy requires proper embryo implantation. Low implantation rate is a major problem during infertility treatments using assisted reproductive technologies<sup>1</sup>. Here we report a newly discovered molecular influence on implantation through the lysophosphatidic acid (LPA) receptor LPA<sub>3</sub> (refs 2–4). Targeted deletion of LPA<sub>3</sub> in mice resulted in significantly reduced litter size, which could be attributed to delayed**

**implantation and altered embryo spacing. These two events led to delayed embryonic development, hypertrophic placentas shared by multiple embryos and embryonic death. An enzyme demonstrated to influence implantation, cyclooxygenase 2 (COX2) (ref. 5), was downregulated in LPA<sub>3</sub>-deficient uteri during pre-implantation. Downregulation of COX2 led to reduced levels of prostaglandins E<sub>2</sub> and I<sub>2</sub> (PGE<sub>2</sub> and PGI<sub>2</sub>), which are critical for implantation<sup>1</sup>. Exogenous administration of PGE<sub>2</sub> or carbaprostacyclin (a stable analogue of PGI<sub>2</sub>) into LPA<sub>3</sub>-deficient female mice rescued delayed implantation but did not rescue defects in embryo spacing. These data identify LPA<sub>3</sub> receptor-mediated signalling as having an influence on implantation, and further indicate linkage between LPA signalling and prostaglandin biosynthesis.**

Multiple factors can adversely affect successful pregnancy. Two of these factors are failed synchronization between embryonic and endometrial development during implantation and occurrence of multiple gestations (especially monochorionic gestation), which can result in fetal demise<sup>1,6–9</sup>. These factors are particularly important for the clinical success and efficacy of assisted reproductive technologies. One molecular factor that has been previously implicated in female reproduction is the small, bioactive phospholipid LPA<sup>10</sup>. LPA has a range of influences that are mediated by at least four G-protein-coupled receptors, LPA<sub>1–4</sub> (ref. 2). Deletion of LPA<sub>1</sub> and LPA<sub>2</sub> in mice revealed roles for these receptors in neural development, craniofacial formation, neuropathic pain and altered cellular signalling, but without obvious effects on female reproduction<sup>11–14</sup>. These results suggested that LPA signalling in female reproduction might be mediated by other LPA receptors including LPA<sub>3</sub> (formerly known as Edg7) (refs 3, 4), LPA<sub>4</sub> (ref. 15), unidentified LPA receptor(s), or possibly non-receptor pathways. Towards identifying LPA-dependent mechanisms affecting reproduction, we targeted LPA<sub>3</sub> for deletion. LPA<sub>3</sub> is a receptor with distinct signalling properties and a preference for unsaturated LPA species<sup>2–4</sup>.

Functional deletion of LPA<sub>3</sub> was achieved by replacing a fragment covering the untranslated region and the start codon in exon 2 with a neomycin-resistance gene in reverse orientation in R1 embryonic stem cells (Supplementary Figs 1 and 2). The LPA<sub>3</sub>-deficient mice were born with normal mendelian frequency without sexual bias (Supplementary Table 1), and appeared grossly normal (data not shown). However, LPA<sub>3</sub>-deficient females produced litter sizes of less than 50% compared with that of wild-type and LPA<sub>3</sub> heterozygote controls (Supplementary Table 2), and showed a statistically significant prolongation of pregnancy (20.9 ± 0.5 days versus 19.4 ± 0.7 days in wild-type and LPA<sub>3</sub> heterozygote controls, *P* < 0.05). These phenotypes were independent of stud genotype, indicating defects in female reproduction.

Towards determining whether LPA<sub>3</sub> deletion might directly affect the female reproductive system, expression patterns of LPA<sub>3</sub> messenger RNA were assessed using polymerase chain reaction with reverse transcription (RT–PCR) and *in situ* hybridization. RT–PCR revealed the presence of LPA<sub>3</sub> mRNA in oviduct, placenta and uterus but not in ovary and eggs (unfertilized eggs and fertilized eggs from one cell to pre-implantation blastocyst; data not shown). Within the uterus, LPA<sub>3</sub> mRNA expression was upregulated during postnatal development and varied during the oestrous cycle (Supplementary Fig. 3a, b). Notably, LPA<sub>3</sub> mRNA levels increased during early pregnancy, peaking around embryonic day 3.5 (E3.5) then returning to basal levels from E4.5 through to the end of pregnancy (Fig. 1a). RT–PCR of microdissected E3.5 uterine tissue and *in situ* hybridization indicated that LPA<sub>3</sub> mRNA expression was confined to the luminal endometrial epithelium at E3.5 (Fig. 1b–d; see also Supplementary Fig. 3c). These data suggested that LPA<sub>3</sub> loss of function resulting in reduced litter sizes could involve direct effects on the female reproductive system.

To explore this possibility, we examined major events in female reproduction: from ovulation through to decidualization. No

significant differences were observed in superovulation, fertilization or decidualization between wild-type or LPA<sub>3</sub> heterozygote controls and LPA<sub>3</sub>-deficient female littermates. No significant differences in blastocyst number or developmental stage, isolated from E3.5 uteri, were observed between control and LPA<sub>3</sub>-deficient females. These data indicated no obvious defects in ovulation, ovum transport and blastocyst development in LPA<sub>3</sub>-deficient female mice (Fig. 1e; see also Supplementary Fig. 4).

In contrast, embryo implantation studies identified clear phenotypic changes in LPA<sub>3</sub>-deficient dams: delayed implantation and

altered positioning/crowding of embryos. By E4.5, implantation sites identifiable by Evans blue labelling in control animals were absent in uteri of LPA<sub>3</sub>-deficient dams. Implantation sites became detectable at E5.5 in uteri of LPA<sub>3</sub>-deficient mice (Fig. 1f, g)<sup>16</sup>. The number of pre-implantation blastocysts recovered from E4.5 LPA<sub>3</sub>-deficient uteri was comparable to that from E3.5 control and LPA<sub>3</sub>-deficient uteri (Fig. 1e), indicating that delayed implantation in uteri of LPA<sub>3</sub>-deficient mice was due to extra-embryonic influences of LPA signalling. In addition to delayed implantation, LPA<sub>3</sub>-deficient uteri had a reduced number of implantation sites compared with that in the control uteri, despite the fact that comparable numbers of blastocysts were available for implantation. The implantation sites in the LPA<sub>3</sub>-deficient uteri were crowded/clustered in the uterine segments proximal to the cervix (Fig. 1g). This aberrant crowding of embryos in uteri of LPA<sub>3</sub>-deficient mice was further demonstrated by findings at later gestational stages. At E10.5, 44% of implantation sites in LPA<sub>3</sub>-deficient uteri contained two to four embryos (averaging 1.65 live embryos per implantation site) (Fig. 2a, b). At E18.5, 28% of placentas were shared by two to

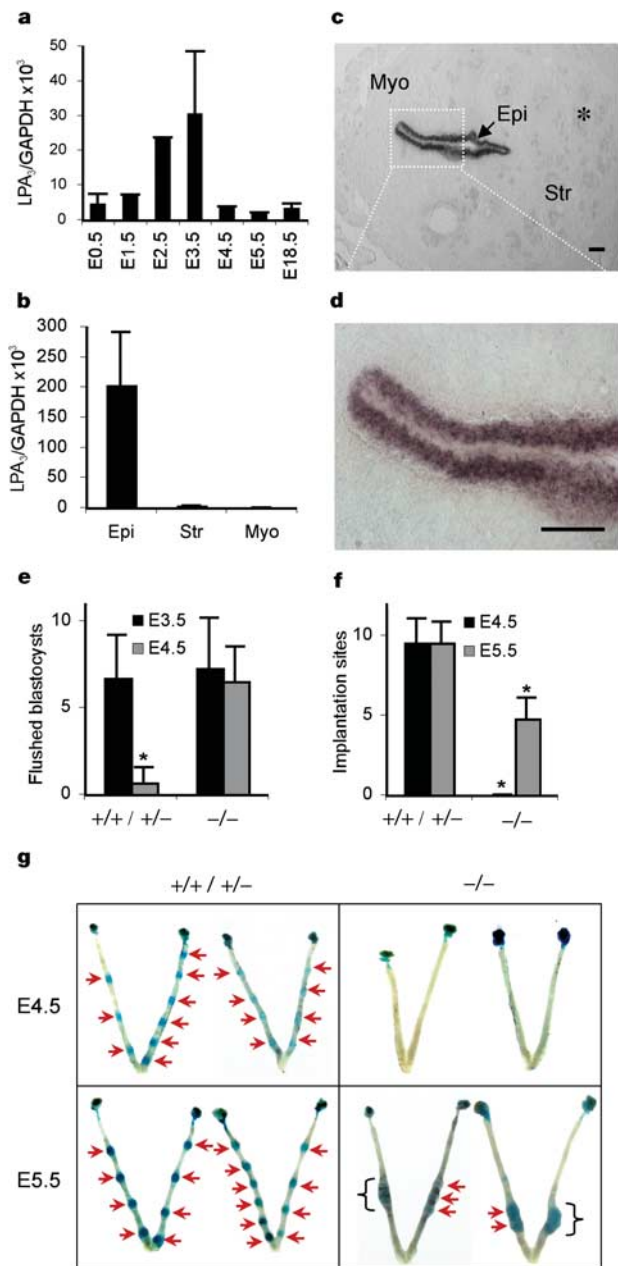


**Figure 1** LPA<sub>3</sub> mRNA expression in wild-type uterus and effects of LPA<sub>3</sub> deficiency on implantation. **a, b**, Quantification of uterine LPA<sub>3</sub> mRNA during pregnancy (**a**) and in E3.5 luminal endometrial epithelium (Epi), stroma (Str) and myometrium (Myo) (**b**). **c, d**, *In situ* localization of LPA<sub>3</sub> in E3.5 wild-type uterus. The asterisk indicates glandular endometrial epithelium. Scale bars: 100  $\mu$ m. **e**, Number of flushed blastocysts from E3.5 and E4.5 uteri. **f, g**, Number (**f**) and location (**g**) of implantation sites at E4.5 and E5.5 uteri. Blue bands (arrows) indicate implantation sites; brackets indicate clustered implantation sites. Asterisk,  $P < 0.001$ . In all figures, error bars are standard deviations. +/+, +/- and -/- represent wild-type, heterozygote and LPA<sub>3</sub>-deficient mice, respectively.

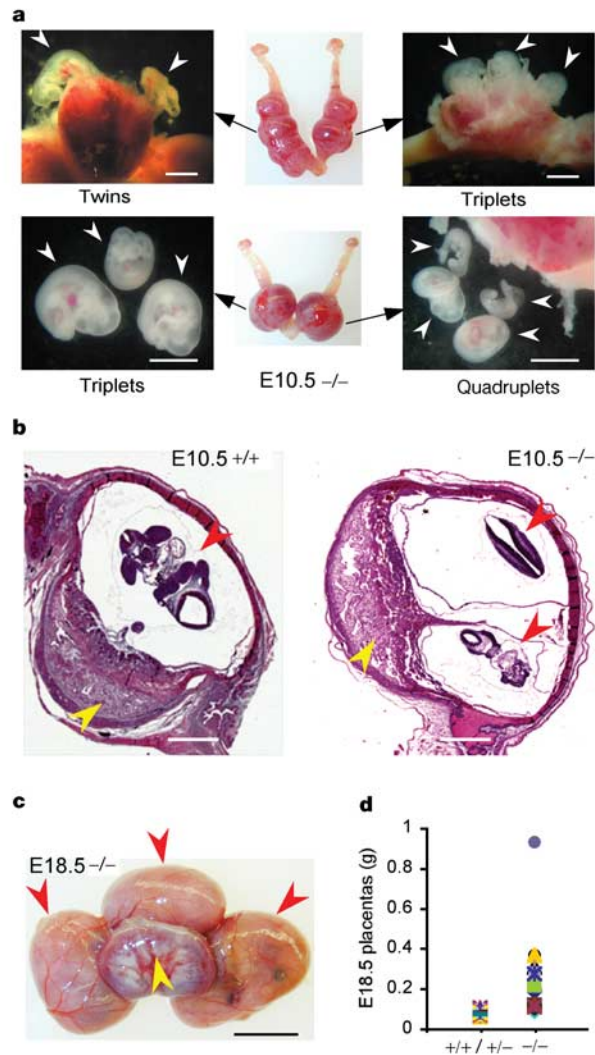


**Figure 2** Multiple embryos at individual implantation sites and placental hypertrophy in uteri of LPA<sub>3</sub>-deficient mice. **a**, Samples of multiple embryos at individual implantation sites at E10.5. White arrowheads indicate embryos. Scale bars: 2 mm. **b**, Cross-sections of E10.5 uteri revealing two less-developed embryos sharing one placenta in a LPA<sub>3</sub>-deficient uterus. Scale bars: 1 mm. **c**, A placenta shared by three embryos at E18.5 in a LPA<sub>3</sub>-deficient uterus. Scale bar: 8 mm. Red arrowheads in **b** and **c** indicate embryos; yellow arrowheads indicate placentas. **d**, Weight of placentas at E18.5.

## letters to nature

three embryos (Fig. 2c) and associated with placental hypertrophy (Fig. 2d; see also Supplementary Fig. 5). These phenomena were never observed in controls.

In addition, embryos isolated from LPA<sub>3</sub>-deficient uteri (at E10.5 and E18.5) were always smaller than those from wild-type or LPA<sub>3</sub> heterozygote controls at comparable ages (Fig. 3a–c), although newborns from LPA<sub>3</sub>-deficient females were, on average, heavier (Fig. 3c), possibly resulting from prolonged pregnancy and/or smaller litter size. The average number of live embryos per animal that could be isolated from LPA<sub>3</sub>-deficient females decreased after initial implantation (Fig. 3d). Delayed implantation and aberrant embryo spacing were thus associated with both delayed embryonic development and embryonic death, which could account for the reduced litter sizes produced by LPA<sub>3</sub>-deficient females.

To determine whether LPA<sub>3</sub> loss in the embryo itself might contribute to the phenotypes, embryo transfer experiments were pursued. Wild-type blastocysts were transferred to wild-type or LPA<sub>3</sub>-deficient pseudo-pregnant uteri. Transferred wild-type embryos in wild-type or LPA<sub>3</sub>-deficient pseudo-pregnant uteri were phenotypically indistinguishable for implantation and development compared to embryos produced by natural matings in wild-type or LPA<sub>3</sub>-deficient animals. Similarly, when LPA<sub>3</sub>-deficient blastocysts were transferred to wild-type pseudo-pregnant uteri, no implantation or spacing abnormalities were observed (Supplementary Fig. 6 and data not shown). Wild-type and LPA<sub>3</sub>-deficient blastocysts had comparable implantation rates in

wild-type pseudo-pregnant uteri. Considering the fact that no LPA<sub>3</sub> mRNA was detected in wild-type pre-implantation blastocysts, these results eliminate significant contributions of LPA<sub>3</sub> via pre-/post-implantation embryos, and indicate that maternal LPA<sub>3</sub> signalling is responsible for the observed phenotypes.

The observed implantation phenotypes of LPA<sub>3</sub>-deficient mice were markedly similar to those reported for rats and mice treated with indomethacin<sup>17,18</sup>, and for mice deficient in cytosolic phospholipase A<sub>2α</sub> (cPLA<sub>2α</sub>)<sup>19</sup>. Indomethacin is an inhibitor of cyclooxygenases<sup>20</sup>, which convert arachidonic acid to prostaglandin H<sub>2</sub> (PGH<sub>2</sub>) in the biosynthesis of prostaglandins, whereas cPLA<sub>2α</sub> is an important enzyme producing arachidonic acid. Notably, COX2 deficiency, but not COX1 deficiency, in mice results in multiple female reproductive failures, including implantation defects<sup>5,21</sup>, although the precise phenotypes can be influenced by genetic background<sup>22,23</sup>. Moreover, PGE<sub>2</sub> and carbaprostacyclin (cPGI, a stable analogue of PGI<sub>2</sub>) can partially correct implantation defects in both cPLA<sub>2α</sub>-deficient and COX2-deficient mice<sup>19,24</sup>. These data indicate that the cPLA<sub>2α</sub>-arachidonic acid-COX-prostaglandin pathway is crucial for implantation<sup>1</sup>. In view of the phenotypic similarities between LPA<sub>3</sub> deficiency and cPLA<sub>2α</sub>/prostaglandin

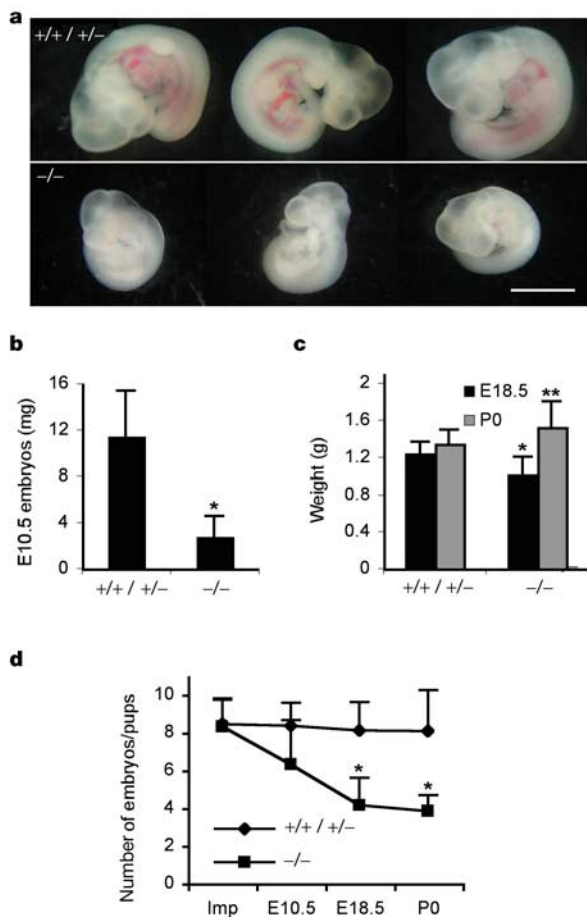


**Figure 3** Delayed post-implantational development of embryos and increased embryonic death in uteri of LPA<sub>3</sub>-deficient mice. **a**, Representative embryos from E10.5 uteri. Scale bar: 2 mm. **b**, E10.5 embryo weight. **c**, Weights of E18.5 embryos and postnatal day 0 (P0) pups. **d**, The average numbers of embryos implanted (Imp), at E10.5 and E18.5, and P0 pups. The numbers of embryos implanted were calculated as described in Methods. Asterisk,  $P < 0.001$ ; double asterisk,  $P < 0.05$ .

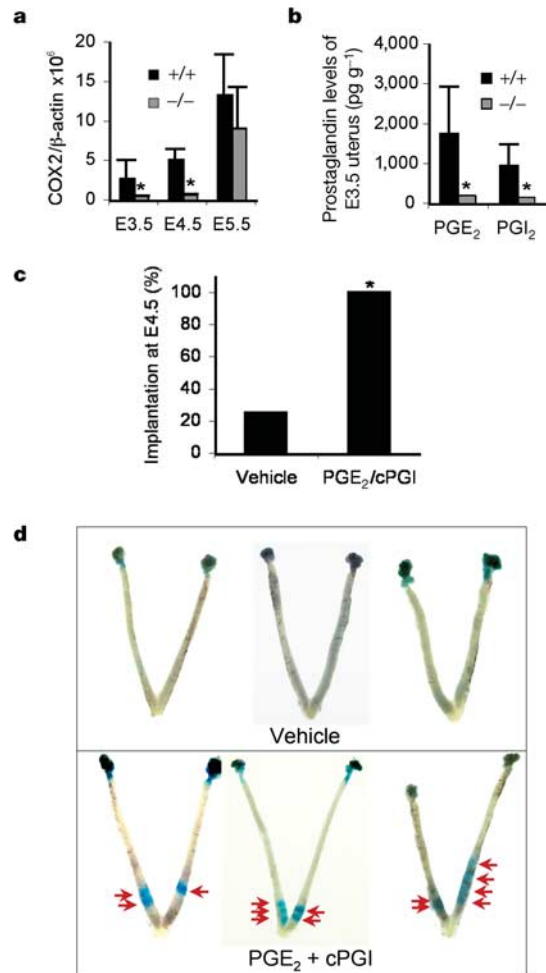


**Figure 4** Reduced COX2 mRNA and prostaglandin levels in uteri of LPA<sub>3</sub>-deficient mice, and exogenous prostaglandin rescue of delayed implantation. **a**, Expression of COX2 during early pregnancy in wild-type and LPA<sub>3</sub>-deficient uteri. Asterisk,  $P < 0.05$ . **b**, Reduced PGE<sub>2</sub> and PGI<sub>2</sub> levels in E3.5 LPA<sub>3</sub>-deficient uteri. Asterisk,  $P < 0.05$ . **c**, Significantly increased percentage of LPA<sub>3</sub>-deficient female mice showing on-time implantation upon PGE<sub>2</sub> and cPGI (a stable PGI<sub>2</sub> analogue) treatment at E3.5. Asterisk,  $P = 0.003$ . **d**, Images of E4.5 LPA<sub>3</sub>-deficient uteri with or without prostaglandin treatment. Red arrows indicate implantation sites.

deficiency, we proposed that LPA<sub>3</sub> might converge on this signalling pathway.

Components of prostaglandin signalling were therefore examined in uteri of LPA<sub>3</sub>-deficient mice. These components included cPLA<sub>2α</sub>, COX1 and COX2, and G-protein-coupled prostaglandin E<sub>2</sub> receptors EP<sub>1-4</sub> and prostaglandin I<sub>2</sub> receptor, IP<sub>25</sub>, along with leukaemia inhibitory factor (LIF) and Hoxa-10, two key regulators in implantation<sup>1</sup>. Only COX2 mRNA levels were significantly reduced in LPA<sub>3</sub>-deficient uteri (Fig. 4a, Supplementary Fig. 7, and data not shown). COX2 is a rate-limiting enzyme for prostaglandin biosynthesis. Consistent with this function, the suppression of COX2 expression in E3.5 LPA<sub>3</sub>-deficient uteri resulted in reduced production of PGE<sub>2</sub> and PGI<sub>2</sub> (Fig. 4b), leading to conditions that are inadequate for implantation, which normally occurs around E4.0 (refs 18, 26). To rescue this prostaglandin reduction, we delivered exogenous PGE<sub>2</sub> and cPGI to E3.5 LPA<sub>3</sub>-deficient female mice, a general approach previously reported<sup>19</sup>. After prostaglandin exposure, significantly more LPA<sub>3</sub>-deficient female mice with normal (on-time) implantation were detected compared with LPA<sub>3</sub>-deficient females given vehicle controls (Fig. 4c,  $P = 0.003$ ). Notably, this rescue did not affect the uneven embryo spacing nor completely restore the reduction of implantation sites compared with wild-type controls (Figs 1g and 4d).

These findings identify LPA signalling as having an influence on embryo implantation, and are the first to link a lysophospholipid G-protein-coupled receptor to prostaglandin biosynthesis, thereby influencing female fertility. As a class, lysophospholipid receptors represent a 'drugable' target, as demonstrated by the compound FTY720, which is currently in phase III clinical trials for prevention of transplantation rejection<sup>27</sup>. This raises the possibility of creating medicines that influence implantation timing, a critical factor for *in vitro* fertilization<sup>1,9</sup> and also for reducing the incidence of multi-embryo gestations, especially monochorionic gestations, which can result in fetal demise<sup>6</sup>. The reduced litter sizes observed in receptor-null mutants for another lysophospholipid, sphingosine 1-phosphate, suggest that other lysophospholipid receptors may also influence mammalian reproduction through pharmacologically tractable mechanisms<sup>28</sup>. □

## Methods

### Quantitative RT-PCR

Primers used were as described<sup>11,12,29</sup>. For amplification of COX2, the following primers were used: forward 5'-AAGCGAGGACCTGGGTTCA-3'; reverse, 5'-AAGCGCGAGTTTATGTTGCTGT-3'. Quantitative RT-PCR was performed as described<sup>29</sup>. The transcript number of target genes was quantified and normalized against GAPDH or β-actin transcript number.

### In situ hybridization and histology

The animals were anaesthetized with halothane inhalation followed by cervical dislocation. *In situ* hybridization and histology were performed as described<sup>30</sup>. Sense and antisense DIG-labelled cRNA probes were generated using appropriate polymerases from a full-length murine LPA<sub>3</sub> complementary DNA.

### Mating, embryo collection and implantation localization

All the mice used in this study were of mixed background (129/SvJ and C57BL/6). Because no difference was observed for all the parameters examined between wild-type and heterozygote female mice (Supplementary Table 2, Supplementary Fig. 8a, b, and data not shown), females of either wild-type or heterozygote genotypes were used as controls. Females were naturally mated with wild-type stud males. The day a plug was found was designated as E0.5. Plugged females were anaesthetized with halothane inhalation followed by cervical dislocation. Uteri of pregnant females were dissected at E3.5, E4.5, E5.5, E10.5 and E18.5. Embryos at E10.5 were fixed in 10% formalin overnight before being weighed. Implantation sites at E4.5 and E5.5 were localized by intravenous injection of Evans blue dye (200 μl, 1% in 1 × PBS, Sigma)<sup>16</sup>. The number of embryos initially implanted in LPA<sub>3</sub>-deficient and wild-type and heterozygote uteri were retrospectively calculated from E10.5 as follows: at E10.5, embryos in an average of 1.2 implantation sites (out of a total of 5.0) were absorbed in LPA<sub>3</sub>-deficient uteri, but embryos in only 0.09 implantation sites (out of a total of 8.4) were absorbed in wild-type and heterozygote uteri ( $P = 1.7 \times 10^{-5}$ ). With an average of 1.65 live embryos per implantation site in LPA<sub>3</sub>-deficient uteri and 1.0 live embryo per implantation site in wild-type and heterozygote uteri at E10.5, the total number of embryos initially implanted should be 8.3 ((3.8

live + 1.2 absorbed) × 1.65) in LPA<sub>3</sub>-deficient uteri and 8.4 ((8.31 live + 0.09 absorbed) × 1.0) in wild-type and heterozygote uteri.

### Prostaglandin measurement

Uteri from E3.5 wild-type or LPA<sub>3</sub>-deficient mice were immediately frozen and crushed in liquid nitrogen. Prostaglandins were extracted by the ethyl acetate extraction method. The prostaglandin levels of each sample were determined using the prostaglandin enzyme-linked immunoassay kit (Cayman Chemical). PGI<sub>2</sub> was measured as 6-keto-PGF<sub>1α</sub>.

### Prostaglandin administration

E3.5 LPA<sub>3</sub>-deficient females were intraperitoneally injected with 100 μl of vehicle (10% ETOH with saline, as control) or 5 μg cPGI and 5 μg PGE<sub>2</sub> (Cayman Chemical, in 10% ETOH with saline) at 10:00 and 18:00. Implantation sites were detected using Evans blue dye at E4.5.

### Data representation

Data are expressed as mean ± s.d. Statistical analyses were done using Student's *t*-test or  $\chi^2$  test. The significance level was set at  $P < 0.05$ .

Received 7 February; accepted 28 February 2005; doi:10.1038/nature03505.

- Dey, S. K. *et al.* Molecular cues to implantation. *Endocr. Rev.* **25**, 341–373 (2004).
- Ishii, I., Fukushima, N., Ye, X. & Chun, J. Lysophospholipid receptors: signaling and biology. *Annu. Rev. Biochem.* **73**, 321–354 (2004).
- Bando, K. *et al.* Molecular cloning and characterization of a novel human G-protein-coupled receptor, EDG7, for lysophosphatidic acid. *J. Biol. Chem.* **274**, 27776–27785 (1999).
- Contos, J. J. & Chun, J. The mouse lp(A3)/Edg7 lysophosphatidic acid receptor gene: genomic structure, chromosomal localization, and expression pattern. *Gene* **267**, 243–253 (2001).
- Lim, H. *et al.* Multiple female reproductive failures in cyclooxygenase 2-deficient mice. *Cell* **91**, 197–208 (1997).
- Cleary-Goldman, J. & D'Alton, M. Management of single fetal demise in a multiple gestation. *Obstet. Gynecol. Surv.* **59**, 285–298 (2004).
- Umstad, M. P. & Gronow, M. J. Multiple pregnancy: a modern epidemic? *Med. J. Aust.* **178**, 613–615 (2003).
- Daniel, Y. *et al.* Analysis of 104 twin pregnancies conceived with assisted reproductive technologies and 193 spontaneously conceived twin pregnancies. *Fertil. Steril.* **74**, 683–689 (2000).
- Wilcox, A. J., Baird, D. D. & Weinberg, C. R. Time of implantation of the conceptus and loss of pregnancy. *N. Engl. J. Med.* **340**, 1796–1799 (1999).
- Tokumura, A., Fukuzawa, K., Yamada, S. & Tsukatani, H. Stimulatory effect of lysophosphatidic acids on uterine smooth muscles of non-pregnant rats. *Arch. Int. Pharmacodyn. Ther.* **245**, 74–83 (1980).
- Contos, J. J., Fukushima, N., Weiner, J. A., Kaushal, D. & Chun, J. Requirement for the lpA1 lysophosphatidic acid receptor gene in normal suckling behavior. *Proc. Natl Acad. Sci. USA* **97**, 13384–13389 (2000).
- Contos, J. J. *et al.* Characterization of lpA<sub>2</sub> (Edg4) and lpA<sub>1</sub>/lpA<sub>2</sub> (Edg2/Edg4) lysophosphatidic acid receptor knockout mice: signaling deficits without obvious phenotypic abnormality attributable to lpA<sub>2</sub>. *Mol. Cell. Biol.* **22**, 6921–6929 (2002).
- Kingsbury, M. A., Rehen, S. K., Contos, J. J., Higgins, C. M. & Chun, J. Non-proliferative effects of lysophosphatidic acid enhance cortical growth and folding. *Nature Neurosci.* **6**, 1292–1299 (2003).
- Inoue, M. *et al.* Initiation of neuropathic pain requires lysophosphatidic acid receptor signaling. *Nature Med.* **10**, 712–718 (2004).
- Noguchi, K., Ishii, S. & Shimizu, T. Identification of p2y9/GPR23 as a novel G protein-coupled receptor for lysophosphatidic acid, structurally distant from the Edg family. *J. Biol. Chem.* **278**, 25600–25606 (2003).
- Paria, B. C., Huet-Hudson, Y. M. & Dey, S. K. Blastocyst's state of activity determines the "window" of implantation in the receptive mouse uterus. *Proc. Natl Acad. Sci. USA* **90**, 10159–10162 (1993).
- Kennedy, T. G. Evidence for a role for prostaglandins in the initiation of blastocyst implantation in the rat. *Biol. Reprod.* **16**, 286–291 (1977).
- Kinoshita, K. *et al.* Involvement of prostaglandins in implantation in the pregnant mouse. *Adv. Prostaglandin Thromboxane Leukot. Res.* **15**, 605–607 (1985).
- Song, H. *et al.* Cytosolic phospholipase A2α is crucial for 'on-time' embryo implantation that directs subsequent development. *Development* **129**, 2879–2889 (2002).
- Frenkian, M., Segond, N., Pidoux, E., Cohen, R. & Jullienne, A. Indomethacin, a COX inhibitor, enhances 15-PGDH and decreases human tumoral C cells proliferation. *Prostaglandins* **65**, 11–20 (2001).
- Reese, J., Brown, N., Paria, B. C., Morrow, J. & Dey, S. K. COX-2 compensation in the uterus of COX-1 deficient mice during the pre-implantation period. *Mol. Cell. Endocrinol.* **150**, 23–31 (1999).
- Sibilia, M. & Wagner, E. F. Strain-dependent epithelial defects in mice lacking the EGF receptor. *Science* **269**, 234–238 (1995).
- Wang, H. *et al.* Rescue of female infertility from the loss of cyclooxygenase-2 by compensatory up-regulation of cyclooxygenase-1 is a function of genetic makeup. *J. Biol. Chem.* **279**, 10649–10658 (2004).
- Lim, H. *et al.* Cyclo-oxygenase-2-derived prostacyclin mediates embryo implantation in the mouse via PPARδ. *Genes Dev.* **13**, 1561–1574 (1999).
- Yang, Z. M. *et al.* Potential sites of prostaglandin actions in the periimplantation mouse uterus: differential expression and regulation of prostaglandin receptor genes. *Biol. Reprod.* **56**, 368–379 (1997).
- Paria, B. C., Song, H. & Dey, S. K. Implantation: molecular basis of embryo-uterine dialogue. *Int. J. Dev. Biol.* **45**, 597–605 (2001).
- Gabardi, S. & Cerio, J. Future immunosuppressive agents in solid-organ transplantation. *Prog. Transplant.* **14**, 148–156 (2004).
- Ishii, I. *et al.* Marked perinatal lethality and cellular signaling deficits in mice null for the two sphingosine 1-phosphate (S1P) receptors, S1P<sub>2</sub>/LPB<sub>2</sub>/EDG-5 and S1P<sub>1</sub>/LPB<sub>1</sub>/EDG-3. *J. Biol. Chem.* **277**, 25152–25159 (2002).
- Hama, K. *et al.* Lysophosphatidic acid and autotaxin stimulate cell motility of neoplastic and non-neoplastic cells through LPA1. *J. Biol. Chem.* **279**, 17634–17639 (2004).

30. Ishii, I. *et al.* Selective loss of sphingosine 1-phosphate signaling with no obvious phenotypic abnormality in mice lacking its G protein-coupled receptor, LP<sub>β3</sub>/EDG-3. *J. Biol. Chem.* **276**, 33697–33704 (2001).

Supplementary Information accompanies the paper on [www.nature.com/nature](http://www.nature.com/nature).

**Acknowledgements** We thank F. Liu, S. Kupriyanov, R. Rivera, D. Herr, E. Nilsson, M. Murakami, Y. Kita, B. C. Paria, C. Akita, S. Carlson and Q. Chen for technical assistance and suggestions. This work was supported by grants from the National Institute of Mental Health to J.C. and J.J.A.C., the National Institute of Health to M.K.S, Swiss National Science Foundation to B.A., and Program for Promotion of Fundamental Studies in Health Sciences of the Pharmaceuticals and Medical Devices Agency (PMDA) and grants-in-aid from the Ministry of Education, Science, Culture and Sports for the 21st Century Center of Excellence Program, Japan, to H.S., J.A and H.A.

**Competing interests statement** The authors declare that they have no competing financial interests.

**Correspondence** and requests for materials should be addressed to J.C. ([jchun@scripps.edu](mailto:jchun@scripps.edu)).

## Cellular APOBEC3G restricts HIV-1 infection in resting CD4<sup>+</sup> T cells

Ya-Lin Chiu<sup>1</sup>, Vanessa B. Soros<sup>1</sup>, Jason F. Kreisberg<sup>1,2</sup>, Kim Stopak<sup>1,2</sup>, Wes Yonemoto<sup>1</sup> & Warner C. Greene<sup>1,2</sup>

<sup>1</sup>Gladstone Institute of Virology and Immunology, <sup>2</sup>Departments of Medicine, Microbiology and Immunology, University of California, San Francisco, California 94143, USA

In contrast to activated CD4<sup>+</sup> T cells, resting human CD4<sup>+</sup> T cells circulating in blood are highly resistant to infection with human immunodeficiency virus (HIV)<sup>1–4</sup>. Whether the inability of HIV to infect these resting CD4<sup>+</sup> T cells is due to the lack of a key factor, or alternatively reflects the presence of an efficient mechanism for defence against HIV, is not clear. Here we show that the anti-retroviral deoxycytidine deaminase APOBEC3G<sup>5</sup> strongly protects unstimulated peripheral blood CD4<sup>+</sup> T cells against HIV-1 infection. In activated CD4<sup>+</sup> T cells, cytoplasmic APOBEC3G resides in an enzymatically inactive, high-molecular-mass (HMM) ribonucleoprotein complex that converts to an enzymatically active low-molecular-mass (LMM) form after treatment with RNase. In contrast, LMM APOBEC3G predominates in unstimulated CD4<sup>+</sup> T cells, where HIV-1 replication is blocked and reverse transcription is impaired<sup>1–3</sup>. Mitogen activation induces the recruitment of LMM APOBEC3G into the HMM complex, and this correlates with a sharp increase in permissivity for HIV infection in these stimulated cells. Notably, when APOBEC3G-specific small interfering RNAs are introduced into unstimulated CD4<sup>+</sup> T cells, the early replication block encountered by HIV-1 is greatly relieved. Thus, LMM APOBEC3G functions as a potent post-entry restriction factor for HIV-1 in unstimulated CD4<sup>+</sup> T cells. Surprisingly, sequencing of the reverse transcripts slowly formed in unstimulated CD4<sup>+</sup> T cells reveals only low levels of dG → dA hypermutation, raising the possibility that the APOBEC3G-restricting activity may not be strictly dependent on deoxycytidine deamination.

APOBEC3G belongs to a family of tissue-restricted (deoxy)cytidine deaminases<sup>6</sup> that edit RNA and mutates DNA<sup>6,7</sup>. In the case of HIV, the incorporation of APOBEC3G into virions leads to extensive mutation of nascent HIV DNA formed during reverse transcription in the next round of infection<sup>5,8–11</sup>. The Vif protein of HIV circumvents this anti-HIV defence mechanism by enhancing the 26S proteasome-mediated degradation of APOBEC3G<sup>12–14</sup> and decreasing its synthesis<sup>12,15</sup>. These events make APOBEC3G

unavailable for incorporation into budding virions, and thus, its anti-retroviral action is forfeited.

One puzzling aspect of APOBEC3G biology is why cytoplasmic forms of this enzyme in target CD4<sup>+</sup> T cells undergoing HIV infection fail to recapitulate the antiviral effects of intra-virion APOBEC3G. Perhaps cellular APOBEC3G is subject to some form of negative regulation. APOBEC1 (ref. 16) and activation-induced cytidine deaminase (AID)<sup>17</sup> are two well-characterized members of this (deoxy)cytidine deaminase family. APOBEC1 is the central component of an RNA-editing complex and is regulated by its assembly with APOBEC1-complementing factor<sup>16</sup>. AID catalyses the deamination of dC residues, yielding dU on single-stranded DNA *in vitro*, but has no measurable deaminase activity unless pre-treated with RNase to remove small inhibitory RNAs bound to AID<sup>18</sup>. These findings prompted us to determine whether APOBEC3G assembles into HMM complexes and to assess the potential role of RNA binding in the regulation of APOBEC3G.

Proteins in lysates of H9 T cells harbouring endogenous APOBEC3G were size fractionated by gel filtration on a Superose 6HR 10/30 column using a fast performance liquid chromatography (FPLC) apparatus followed by SDS–polyacrylamide gel electrophoresis (PAGE) and anti-APOBEC3G immunoblotting of the individual fractions. The endogenous ~46-kDa APOBEC3G enzyme resided principally in a HMM complex that is >700 kDa in mass (Fig. 1a, top). However, when lysates were treated with

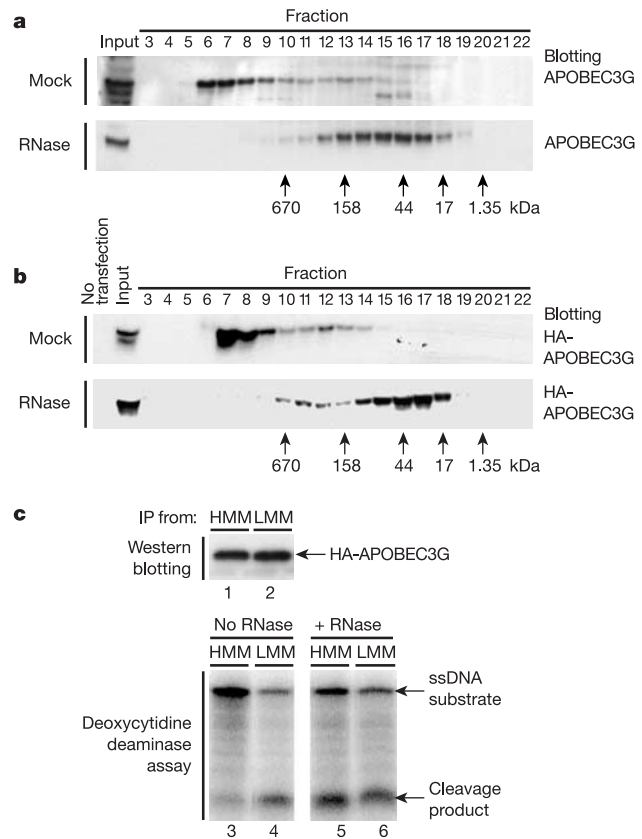


**Figure 1** APOBEC3G is negatively regulated by recruitment into an enzymatically inactive HMM complex. **a, b**, Endogenous APOBEC3G in human H9 T cells (**a**) and exogenous HA-APOBEC3G expressed in 293T cells (**b**) reside principally in >700-kDa HMM complexes that can be converted to LMM forms after RNase A treatment. **c**, HMM (top, fractions 7–9) and LMM (bottom, fractions 15–17) forms of HA-APOBEC3G resolved by FPLC were immunoprecipitated (IP) with anti-HA (Covance), and HA-APOBEC3G protein content was assessed by anti-APOBEC3G antibody (lanes 1 and 2). The immunoprecipitates were tested in a deoxycytidine deaminase assay with or without RNase treatment. ssDNA, single-stranded DNA.